

Steps and Gaps in Ground Ruptures: Empirical Bounds on Rupture Propagation

by Glenn P. Biasi and Steven G. Wesnousky*

Abstract We analyze a set of 76 mapped surface ruptures for relationships between geometrical discontinuities in fault traces and earthquake rupture extent. The combined set includes 46 strike-slip, 16 normal, and 14 reverse mechanism events. The survey shows ~90% of ruptures have at least one end at a mappable discontinuity, either a fault end or a step of 1 km or greater. Dip-slip ruptures cross larger steps than strike-slip earthquakes, with maxima of ~12 versus ~5 km, respectively. Large steps inside strike-slip ruptures are rare; only 8% (5 of 62) are ≥ 4 km. A geometric probability distribution model of steps as “challenges” to rupture propagation predicts that steps of 1 km or greater will be effective in stopping rupture about 46% of the time. The rate is similar for dip-slip earthquakes, but, within this set, steps are relatively more effective in stopping reverse ruptures and less effective in stopping normal ruptures. By comparing steps at rupture terminations to the set of steps broken in rupture, we can estimate the importance of step size for stopping rupture. We define the passing ratio for a given step size as the fraction of steps broken divided by the corresponding fraction that stop rupture. A linear model for steps from 1 to 6 km in strike-slip ruptures leads to the passing ratio = $1.89 - 0.31 \times \text{step width}$. Steps of ~3 km are equally likely to be broken or to terminate rupture, and steps ≥ 6 km should almost always stop rupture. A similar comparison suggests that extensional steps are somewhat more effective than compressional steps in stopping ruptures. We also compiled the incidence of gaps of 1 km and longer in surface ruptures. Gaps occur in ~43% of ruptures and occur more frequently in dip-slip than strike-slip ruptures.

Online Material: Figures of annotated surface rupture maps for 40 earthquakes.

Introduction

Regional seismic-hazard analysis today generally begins with the construction of a map of active faults in the area of interest. The fault map shows where large earthquakes are expected in the future but not how much of the fault will rupture because earthquakes do not always rupture the entirety of the fault on which they occur. History shows earthquake ruptures may jump from one fault strand to another. It therefore remains a problem in seismology to estimate the likely length and location of future earthquake ruptures on mapped faults. We here present a global data set (Fig. 1) analyzing 76 surface rupture maps of continental earthquakes. The maps provide a basis to examine whether or not there is a systematic relationship between aspects of fault geometry, primarily the presence of discontinuous steps in fault traces, and the length to which earthquakes

will propagate along a fault. The specific aspects we address are:

- the number of geometrical steps in rupture traces versus rupture length;
- the dimension of geometrical steps in a fault trace across which ruptures have propagated;
- prediction of the number of steps in a fault trace across which a fault will rupture;
- the effect of step size on rupture propagation;
- the percentage of ruptures that may be expected to terminate at structural complexities along strike; and
- the presence of gaps in earthquake ruptures along continuous fault traces.

We begin with a description of the data set, follow with a presentation of the analysis and findings, and finish with discussion and conclusion sections that place the findings in the context of recent efforts to develop seismic-hazard maps and physical models describing the process of earthquake rupture propagation.

*Also at Center for Neotectonic Studies, University of Nevada Reno, Mail Stop-169, Reno, Nevada 89557.

Data and Observations

To develop measurements of step and gap incidence and size, we draw upon surface rupture maps and related published literature for the earthquakes listed in Tables 1 and 2. A total of 46 strike-slip ruptures, 16 normal-faulting events, and 14 reverse-faulting events have been synthesized. The 39 events in Table 1 are newly summarized in this work. For each, we have redrafted the surface rupture maps to put them in a common format and to identify features noted in measurements and interpretations. ⑤ Maps and the accompanying information for all new events are available in the electronic supplement to this article. Table 2 summarizes measurements from the previous rupture map collection in Wesnousky (2008). Relative to that collection, Table 1 is comprised of events that postdate it or that came by a more thorough inclusion of events known from other compilations (e.g., Wells and Coppersmith, 1994). New studies of older events, especially in China, also contribute significantly to the event set. As an example, and to illustrate the common format used to display the maps, we show the 1931 Fuyun, China, earthquake in Figure 2. In this case, rupture information for the Fuyun earthquake was developed using a combination of satellite photogrammetric methods and field verification (Shi *et al.*, 1984; Klinger *et al.*, 2011). In the preparation of each map, original descriptions of the events were reviewed for comments pertaining to fault geometry and surface rupture continuity. Each map is further annotated to show the location and size of steps and gaps in rupture in the fault trace, which are the primary focus of this study. Steps are defined as those sites where a rupture or fault trace is interrupted by a discontinuity that may be described as requiring an observer to step approximately orthogonally from the end of a rupture segment to find the continuation of the fault or rupture or their projections along strike (both cases are shown in Fig. 3). The size or dimension of steps is here taken as the distance across the step at the surface. Attention is limited to steps of ~ 1 km or greater, because many rupture maps are not available in sufficient detail to confidently discriminate smaller features. Gaps are noted where mapping is considered adequate to recognize that there was an absence of surface rupture along a continuous fault trace that then resumes somewhere farther along strike. As with steps, we tabulate only gaps of 1 km or greater. Finally, where fault mapping is available, the earthquake rupture maps show whether and how the active trace continues relative to the end of rupture, steps where they are involved in rupture termination, and the locations of nearby active faults.

Our observations for each earthquake are summarized in Tables 1 and 2. Earthquakes in Table 1 are newly developed with this work; events in Table 2 are summarized from Wesnousky (2008). Steps are defined as “internal” if they fall within an earthquake rupture. The next-to-last column shows the number of internal steps for each rupture, followed in parentheses by the sizes of the steps. The last column labeled “Rupture Ends” indicates whether the data allow interpretation of how the rupture ends relative to the main fault and others nearby. Depend-

ing on the earthquake, the fault continuation may be interpreted at one or both ends, or neither. The initial number in the Rupture Ends column indicates the number of rupture ends characterized and the following values in parentheses describe the character of the fault at the rupture ends. Ruptures that end with the fault are indicated in the column with “end”; positive numbers are step sizes in units of kilometers associated with rupture termination; “-” indicates that the fault continues while the rupture ended; and “n.d.” indicates “no data,” the case in which no interpretation is attempted.

An additional column in Tables 1 and 2 lists either the observed number of gaps of one or more kilometers in the rupture trace or “n.d.,” meaning “no data,” where rupture mapping or preservation may not be sufficient to resolve gaps. Numbers in parentheses are the gap size(s) in kilometers. Finally, Tables 1 and 2 list the rupture mechanism, rupture length, a geographic coordinate along strike of the rupture, the name and date of the causative earthquake, and an event number.

⑤ A narrative description for all new maps is provided in the electronic supplement, with supporting information from the original sources on rupture length, seismic moment, and other relevant details. The narratives also summarize interpretations we have gleaned from publications or interpreted from the maps and sources used in map construction. The descriptions also note where data appear incomplete, insufficient for our analysis, or contain apparent contradictions, and how these uncertainties are considered in the following analysis.

Analysis and Findings

Rupture Length Versus the Number of Internal Steps

The number of internal steps in each rupture is plotted in Figure 4 as a function of length on linear and log scales. Mechanisms of events are distinguished by symbol type. The upper plot, with length plotted on a linear scale, shows there is no linear correlation between the number of internal steps and rupture length. The lower log-linear plot suggests that the maximum number of observed steps as a function does tend to increase with rupture length. The increase in the maximum number of steps can be explained if long ruptures gain length by picking up more sections across steps. At the same time, there are other ruptures of similar length across virtually the entire length spectrum that have few or no steps. Comparing between earthquake mechanisms, dip-slip events with a given number of steps tend toward shorter rupture lengths than strike-slip, perhaps indicating dip-slip ruptures more readily include steps or are less likely to stop at steps in the fault trace.

There are two outliers in the data set that deserve mention. The first is the 1987 Edgcombe, New Zealand, normal-faulting event (Fig. 4, event 27, Wesnousky, 2008), which displays five internal steps along a total rupture length of only 15.5 km. This rupture consisted of multiple short and partially overlapping faults that failed together in a common, spatially extensive extensional regime. The second outlier is

Table 1
Measurements from Newly Synthesized Events

Date (yyyy/mm/dd)	Earthquake	Event Number	Latitude (°)	Longitude (°)	Mechanism*	Length (km)	Magnitude	Gaps (Sizes, km)	Size of Internal Steps (km) [†]	Rupture Ends [‡]
1892/02/02	Laguna Salada, Baja, California	38	32.40	-115.60	S	42	7.2	0	0	0 (n.d., n.d.)
1905/07/23	Bulnay, Mongolia	39	49.00	98.00	S	375	8.4	n.d.	0	2 (-, -)
1911/01/03	Chon-Kemin (Kebim), Kyrgyzstan	40	43.50	77.50	R	177	7.7	n.d.	1 (10)	0 (n.d., n.d.)
1915/01/13	Avezzano, Italy	41	42.00	12.50	N	40	7.0	n.d.	2 (4,7)	2 (3, -)
1920/12/16	Haiyuan, China	42	36.60	105.32	S	237	8.3	n.d.	5 (1 E, 1 E, 2 E, 4 E, 5 R)	2 (-, -)
1927/03/07	Tango (Kiaia-Tango), Japan	43	35.80	134.92	S	35	7.0	0	1 (1 E)	1 (end, n.d.)
1928/01/06	Laikipia-Subukia Kenya	44	0.16	35.75	N	40	6.9	0	1 (1)	2 (end, -)
1931/08/10	Fuyun, China	45	46.57	89.97	S	160	7.9	2 (1.5, 2.5)	1 (2 R)	0 (n.d., n.d.)
1932/12/25	Changma, China	46	39.77	96.69	S	149	7.6	4 (1, 1, 2, 3)	2 (3 R, 5 E)	2 (end, 10 R)
1953/03/18	Yenice-Gonen, Turkey	47	40.12	27.62	S	60	7.2	0	2 (1 R, 2 R)	2 (end, 4 E)
1956/02/09	San Miguel, Mexico	48	31.67	-116.10	S	20	6.7	0	0	2 (3 E, 1 R)
1957/12/04	Gobi-Altai, Mongolia	49	45.15	99.21	S	245	8.1	1 (6)	9 (3 E, 2 E, 2 R, 1 E, 1 E, 2 E, 1 R, 1.5 R, 2 E)	0 (n.d., n.d.)
1962/09/01	Buyin Zara (Ipak fault), Iran	50	35.56	49.81	S	103	7.2	2 (10, 8)	3 (4 R, 2.5 E, 3 E)	0 (n.d., n.d.)
1967/01/05	Mogod, Mongolia	51	48.20	102.93	S	48.5	7.1	1 (2)	0	0 (n.d., n.d.)
1968/08/31	Dash-e-Bayaz, Iran	52	34.05	58.96	S	74	7.1	0	1 (1 E)	2 (2 R, -)
1970/03/28	Gediz, Turkey	53	39.17	29.55	N	40	7.2	0	1 (1)	0 (n.d., n.d.)
1977/12/19	Bob-Tangol, Iran	54	30.92	56.41	S	20	5.9	0	0	2 (1.5 E, -)
1978/09/16	Tabas, Iran	55	33.27	57.39	R	95	7.3	3 (3, 6, 7)	1 (8)	1 (n.d., end)
1979/11/27	Khuli-Buniabad, Iran	56	34.06	59.76	S	55	7.0	1 (2)	1 (1 E)	2 (2 R, end)
1980/11/23	Irpinia, Italy	57	40.79	15.31	N	40	6.9	2 (6, 4)	1 (1)	0 (n.d., n.d.)
1981/02/24-25	Gulf of Corinth, Greece	58	38.10	23.17	N	14	6.6	1 (1)	0	2 (-, -)
1981/03/04	Gulf of Corinth, Greece	59	38.20	23.30	N	13	6.4	0	1 (2)	0 (n.d., n.d.)
1986/09/13	Kalamata, Greece	60	37.08	22.18	N	6	5.8	0	0	2 (end, -)
1988/11/06	Lancang, Yunnan, China	61	22.81	99.61	S	35	7.0	0	2 (2 E, 2 R)	0 (n.d., n.d.)
1988/11/06	Geigma, Yunnan, China	62	23.23	99.44	S	24	6.9	0	0	0 (n.d., n.d.)
1988/12/07	Spitak, Armenia	63	40.93	44.11	R	20	6.7	1 (2)	1 (2)	0 (n.d., n.d.)
1990/06/20	Rudbar, Iran	64	37.00	49.19	S	80	7.4	1 (5)	2 (2 R, 2 R)	0 (n.d., n.d.)
1995/05/27	Neftegorsk (Sakhalin), Russia	65	52.60	142.83	S	36	7.0	0	0	2 (end, end)
1997/05/10	Zirkuh, Iran	66	33.83	59.80	S	125	7.2	0	2 (1 E, 1 R)	2 (end, 4 E)
2005/02/22	Dahuyeh (Zarand), Iran	67	30.80	56.65	R	13	6.4	1 (5.5)	0	2 (end, end)
2005/10/08	Kashmir, Pakistan	68	34.35	73.5	R	75	7.6	0	0	0 (n.d., n.d.)
2008/05/12	Wenchuan, China	69	31.50	104.50	R	240	8.0	1 (4.5)	1 (10)	1 (-, n.d.)
2009/12/19	Malawi, Africa	70	-9.90	33.92	N	9	6.0	1.5	0	0 (n.d., n.d.)
2010/04/04	Sierra Mayor-Cuapah, Mexico	71	32.40	-115.50	S	108	7.2	1 (7)	4 (1 R, 1 R, 1 R, 2 R)	1 (n.d., -)
2010/04/14	Yushu, China-1	72	36.20	96.60	S	32	6.8	0	1 (1 E)	2 (6 E, -)
2010/04/14	Yushu, China-2	73	36.30	96.55	S	18	6.1	0	0	2 (6 E, -)
2010/09/04	Darwin, New Zealand	74	-43.56	172.12	S	29.5	7.0	0	1 (1 R)	0 (n.d., n.d.)
2011/04/11	Iwaki, (Fukushima-Hamadori), Japan	75	36.95	140.69	N	29	6.7	0	1 (2)	2 (end, 1.5)

(continued)

Table 1 (Continued)

Date (yyyy/mm/dd)	Earthquake	Event Number	Latitude (°)	Longitude (°)	Mechanism*	Length (km)	Magnitude	Gaps (Sizes, km)	Size of Internal Steps (km) [†]	Rupture Ends [‡]
2014/08/24	Napa, California	76	38.22	-122.31	S	12.5	6.0	0	0	2 (2 R, -)

Event numbers in this table are generally chronological.

*Mechanisms: S, strike slip; N, normal; R, reverse.

[†]For strike-slip ruptures, the sense of step is indicated as E for extensional and R for restraining.

[‡]end: rupture ends at fault end; n.d., no data; -, rupture ends, fault continues; entry, rupture ends at step of size shown (in kilometers); E and R are as for interior steps.

the 1957 Gobi-Altai strike-slip rupture (event 49), with a main trace rupture length of 245 km and nine interior steps (Table 1). In addition to exhibiting twice the number of steps of any similar event, this rupture appears to have occurred in an exceptional stress regime. For example, strike-slip motion on the main trace occurred on an inclined plane and was accompanied by a significant secondary reverse-faulting zone along much of its length.

Rupture Length Versus the Size of Steps

The sizes of steps observed along each rupture are plotted as a function of rupture length in Figure 5. The step sizes are also coded according to earthquake mechanism. Most prominent in the plot is the tendency for dip-slip ruptures to cross larger steps than strike-slip ruptures of comparable lengths and to cross large steps more frequently than strike-slip ruptures. For strike-slip ruptures, the maximum observed step crossed is 5 km. Only 5 of 62 steps (~8%) are 4 km or larger, and only 3% are ≥ 5 km. In contrast, for dip-slip ruptures, 10 of 33 (30%) steps are ≥ 5 km. This difference may be modified in detail by new rupture maps or future earthquake ruptures, but at present the difference does not appear to be an artifact of data selection or analysis. Rather, the observations seem to reflect an intrinsic difference between the mechanisms that makes dip-slip ruptures more capable than strike-slip ruptures of rupturing across large steps. When attention is limited to just the strike-slip events, with a couple of exceptions, there is a tendency for steps of 3 km and larger to be associated with ruptures longer than ~60 km—11 of 15 such steps occur in ruptures of 100 km or more in length. Similar trends are observed when step size is plotted versus earthquake magnitude (Fig. 6); the largest observed steps are generally associated with larger magnitude earthquakes.

Characterizing the Number of Steps in Historical Ruptures

In Table 3, events are summarized by how many internal steps are observed along the rupture trace. Thus, for example in the “Strike slip” row, there are 46 strike-slip earthquakes in the data set with a total of 62 internal steps, or a coarse average of more than one per rupture. The data are subdivided in the subsequent columns to show the number of events with 0, 1, 2, ... steps along a rupture. The data for normal and reverse mechanism earthquake ruptures are shown in subsequent rows. The row labeled “Dip slip” combines the normal and reverse event values.

The strike-slip and dip-slip data of Table 3 are summarized as histograms in Figure 7. This method of presentation was introduced by Wesnousky and Biasi (2011). Each column represents the number of rupture traces containing a given number of steps divided by the total number of ruptures. The vertical axis is thus the fraction of the total number of events with a particular number of internal steps. For both strike slip and dip slip, the histograms show that the fractional number of

Table 2
Measurements from Wesnousky (2008) Events

Date (yyyy/mm/dd)	Earthquake	Event Number	Latitude (°)	Longitude (°)	Mechanism*	Length (km)	Magnitude	Gaps (sizes in kilometers)	Size of Internal Steps (km) [†]	Rupture Ends [‡]
1857/01/09	Ft Tejon, California [§]	1	35.88	-120.50	S	339	7.9	n.d.	1 (1 E)	2 (1 E, -)
1887/05/03	Sonora (Pitacayachi), Mexico [§]	2	30.80	-109.15	N	102	7.5	1 (7)	2 (2, 5)	0 (n.d., n.d.)
1891/10/28	Neo-Dani, Japan	3	35.60	136.60	S	80	7.3	0	2 (3 R, 2 E)	2 (end, end)
1896/08/31	Rikuu, Japan	4	39.50	144.00	R	37	7.2	1 (8)	2 (2, 12)	2 (end, -)
1915/10/02	Pleasant Valley, Nevada	5	40.50	-117.50	N	61	7.3	0	3 (4, 4, 7)	2 (2, end)
1930/11/02	Kita-Izu, Japan	6	35.00	139.00	S	35	6.7	1 (5)	0	2 (end, end)
1939/12/26	Erzincan, Turkey	7	39.77	39.53	S	300	7.7	0	2 (1 E, 4 E)	2 (5 E, -)
1940/05/19	Imperial, California	8	33.22	-115.70	S	60	6.9	0	0	2 (end, end)
1942/12/20	Erbaa-Niksar, Turkey	9	40.67	36.45	S	28	6.8	0	3 (1 E, 2 R, 1 E)	2 (3 E, 10 E)
1943/11/26	Tosya, Turkey	10	41.00	34.00	S	275	7.6	0	3 (1 E, 1 E, 1.5 E)	2 (2 E, 3 E)
1943/09/10	Totooi, Japan	11	35.25	134.00	S	10.5	6.3	1 (3)	1 (2 R)	2 (end, end)
1944/02/01	Gerede-Bolu, Turkey	12	41.50	32.50	S	155	7.4	0	0	2 (2 E, 1 E)
1945/01/13	Mikawa, Japan	13	34.75	136.75	R	4	6.2	0	0	0 (n.d., n.d.)
1954/12/16	Dixie Valley, Nevada	16	39.20	-118.00	N	47	6.8	2 (4, 2)	1 (3)	2 (-, -)
1954/12/16	Fairview Peak, Nevada	15	39.16	-118.21	N	62	7.0	0	4 (2, 10, 3, 1)	2 (5, end)
1959/08/18	Hebgen Lake, Montana	14	44.55	-110.64	N	25	7.0	0	1 (5)	2 (end, 2)
1967/07/22	Mudumu Valley, Turkey	17	40.63	30.74	S	60	6.7	2 (8, 3)	0	2 (5 E, -)
1968/04/09	Borrego Mountain, California	18	33.16	-116.19	S	31	6.1	0	1 (1.5 R)	2 (2.5 R, -)
1971/02/01	San Fernando, California	19	34.41	-118.40	R	15	6.7	2 (3, 1)	1 (1)	2 (1, 3.4)
1979/06/02	Cadoux, Australia	20	-30.78	117.13	R	10	6.1	0	0	0 (n.d., n.d.)
1979/10/15	Imperial Valley, California	21	32.82	-115.65	S	36	6.3	0	0	2 (end, -)
1980/10/10	El Asnam, Algeria	22	36.15	1.42	R	27.3	6.7	1 (1)	0	0 (n.d., n.d.)
1981/07/29	Sirch, Iran	23	29.96	57.77	S	64	6.4	1 (1)	0	2 (1 E, -)
1983/10/28	Borah Peak, Idaho	24	44.09	-113.81	N	34	6.9	1 (5)	1 (4)	2 (-, -)
1986/03/03	Marryat, Australia	25	-26.22	132.82	R	13	5.9	0	0	0 (n.d., n.d.)
1987/03/02	Edgescombe, New Zealand	27	-38.02	176.92	N	15.5	6.3	0	5 (2, 3, 3, 1.5, 3)	2 (-, end)
1987/11/23	Superstition Hills, California	26	33.07	-115.95	S	25	6.2	0	0	2 (9 R, 10 R)
1988/01/22	Tennant Creek, Australia	28	-19.88	133.83	R	30	6.6	0	1 (6)	0 (n.d., n.d.)
1990/07/16	Luzon, Philippines	29	15.72	121.18	S	112	7.6	1 (1)	1 (1 R)	0 (n.d., n.d.)
1992/06/28	Landers, California	30	34.20	-116.52	S	63.2	7.2	0	3 (1.5 E, 2 E, 3 E)	1 (-, n.d.)
1998/03/14	Fandoqa, Iran	31	30.17	57.61	S	25	6.6	1 (1)	1 (1 E)	2 (1.5 E, -)
1999/09/21	Chi-Chi, Taiwan	32	23.82	120.86	R	72	7.4	0	0	2 (end, end)
1999/11/12	Düzce, Turkey	35	40.82	31.23	S	40	7.0	2 (2, 1)	1 (2.5 E)	2 (1.5 E, 8 E)
1999/08/17	Izmit, Turkey	34	40.77	30.00	S	107	7.1	1 (7)	3 (3 E, 2 E, 2.5 E)	2 (1.5 E, -)
1999/10/16	Hector Mine, California	33	34.56	-116.44	S	44	6.9	0	1 (2.5 E)	2 (end, 2 E)
2001/11/14	Kunlun, China	36	35.92	90.54	S	421	7.8	n.d.	1 (3 E)	1 (-, n.d.)
2002/11/03	Denali, Alaska	37	63.50	-146.00	S	341	7.9	0	1 (3 E)	2 (-, 2.5 E)

Event numbers in this table are generally chronological.

*Mechanisms: S, strike slip; N, normal; R, reverse.

†For strike-slip ruptures, the sense of step is indicated as E for extensional and R for restraining.

‡end, rupture ends at fault end; n.d., no data; -, rupture ends, fault continues; entry, rupture ends at step of size shown, km; E, R are as for interior steps.

§Length modified from Wesnousky (2008).

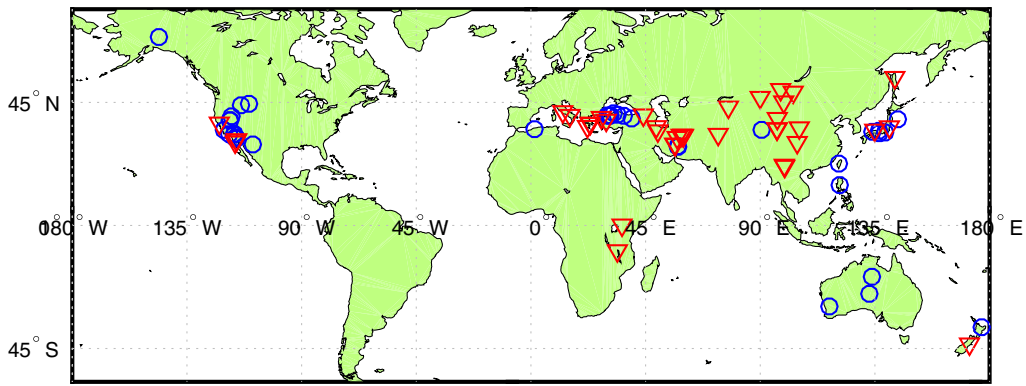


Figure 1. Locations of newly analyzed events (triangles) and previously analyzed events (circles). The color version of this figure is available only in the electronic edition.

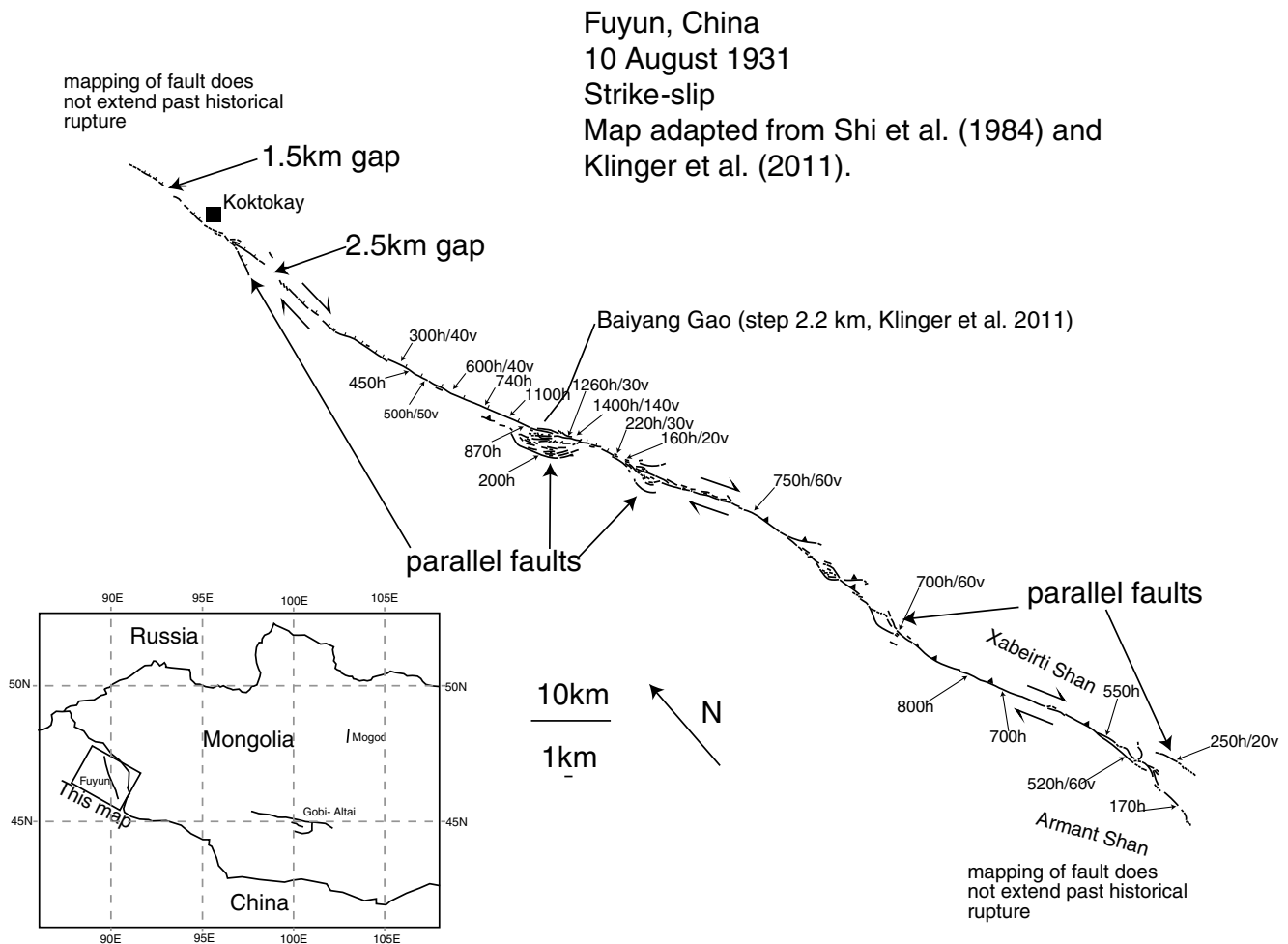


Figure 2. Example surface rupture map, from the 1931 M 7.9 Fuyun, China, earthquake. Details of this event were developed using satellite imagery and field validation (Shi et al., 1984; Klinger et al., 2011; see also Fig. S9).

events decreases as the number of steps increases. The 1957 Gobi-Altai earthquake, with nine interior steps in its main trace and previously described as a distinct outlier, is not included in the strike-slip plot of Figure 7.

To describe the decrease in numbers of events with greater numbers of interior steps, we fit it using a geometric

probability distribution model (Wesnowsky and Biasi, 2011). Steps are viewed as challenges to rupture propagation, with probability p of ending rupture and $q = (1 - p)$ of it continuing. In this model, if X is the random number of trials (steps) k that a rupture encounters, then $k - 1$ steps will be inside the rupture and broken, and one final step succeeds

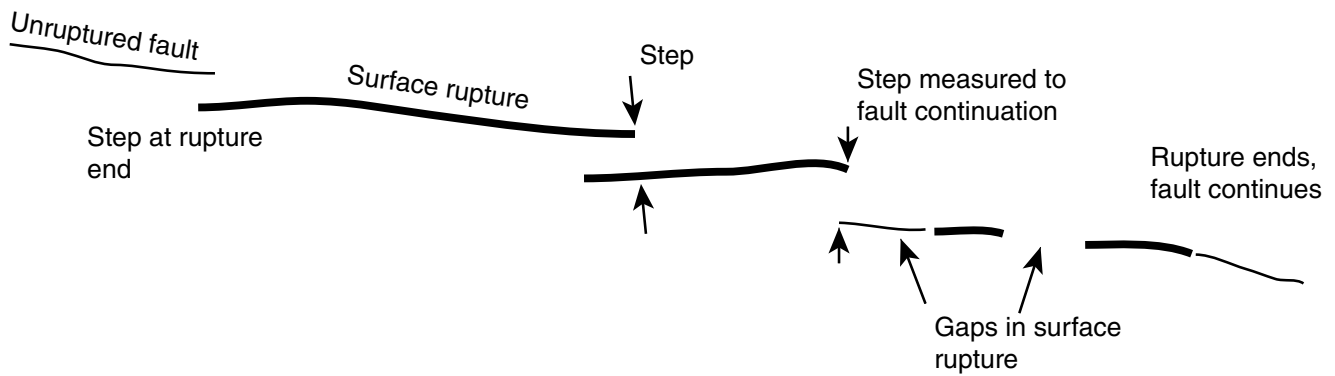


Figure 3. Geometries for measurements made in this article. Heavy lines are surface rupture; thin lines are mapped traces not involved in rupture. Steps are measured at right angles to the fault trace or its continuation at the point of nearest approach. Rupture may end at a step, end although the fault continues, or end with the mapped trace of the fault (not illustrated).

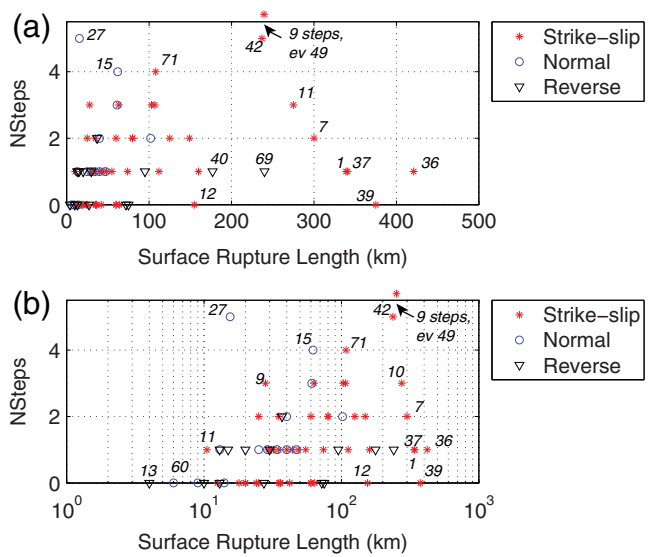


Figure 4. Do longer ruptures continue through more steps? Numbers of steps in ruptures are plotted versus (a) linear and (b) log rupture length. Event numbers are shown for selected events. The 1957 Gobi-Altai event (event 49) would plot above the vertical axis limit. For ruptures longer than about 25 km, there is no clear trend for increasing numbers of steps with rupture length. Dip-slip mechanism ruptures of a given length have more steps in them than do strike-slip events. The color version of this figure is available only in the electronic edition.

in stopping rupture. In treating rupture ends, the geometric model makes two approximations. The rupture ending approximation is readily explained: not all ruptures are actually stopped by steps. Less obvious is that the rupture start is treated as a given, so whether or not it occurs at a step is not considered. The first overestimates trials, whereas the second necessarily underestimates them. The net effect in our case is to approximately cancel out. Assuming the approximate applicability of the geometric model, X is described by probabilities $P_X(k) = pq^{k-1}$, $k = 1, 2, 3, \dots$ and known as a geometric random variable. We use a maximum likelihood method (e.g., Larson, 1982) to find the best estimate of p

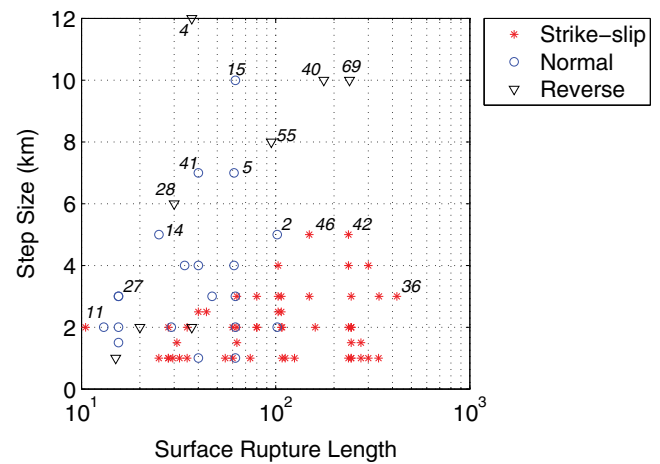


Figure 5. Step size within ruptures versus surface rupture length. Event numbers are indicated for selected events. Events with no steps in their ruptures are not shown. Reverse and normal mechanism ruptures of any given length overcome larger steps than strike-slip ruptures. They cross larger steps, up to 12 km, and cross large steps more frequently than do strike-slip ruptures. Length dependence is observed in maximum step sizes crossed by strike-slip faults. Among these data, if a step of four or more kilometers is crossed in strike slip, it happens in a rupture of 100 km or more. The color version of this figure is available only in the electronic edition.

and its 95% uncertainty range. The results are summarized in Table 4 and shown by the curves plotted in Figure 7. For the strike-slip set, $p = 0.46$ ($0.36 \leq p \leq 0.56$) (Fig. 7 and Table 4). Thus, if steps of 1 km or greater in strike-slip ruptures are considered as a group, they are predicted to stop rupture about 46% of the time (asterisk above the 0 internal step bar [$k = 1$] in Fig. 7). For $k = 2$ trials, $P_X(2) = (0.46)(1 - 0.46) = 0.25$, and so on. For the combined set of dip-slip mechanism ruptures, we also find $p = 0.46$, but with a slightly larger uncertainty range of $0.33 \leq p \leq 0.58$. We show in Figure 8 the dip-slip events separated into normal and reverse types. A greater relative effectiveness of steps to stop reverse ruptures appears likely (Table 4): the best-estimate parameter for reverse ruptures falls outside the

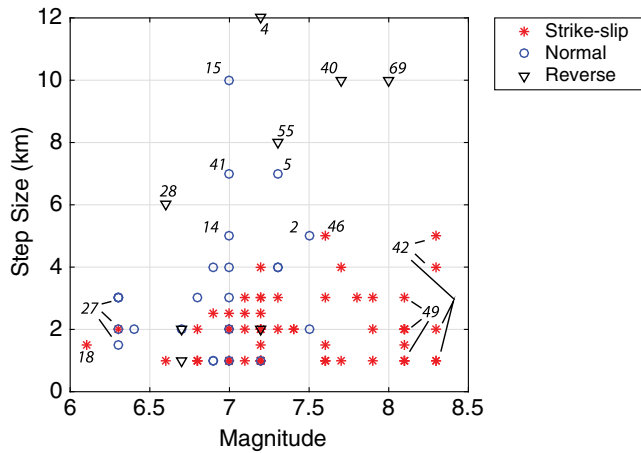


Figure 6. Do larger magnitude events cross larger steps? Magnitude dependence is observed at least in the largest steps passed in ruptures. Ruptures through steps of 4 km all exceed M 7.2, and the smallest-magnitude event crossing a given step size decreases with step size. For a given magnitude, dip-slip ruptures cross larger steps than do strike-slip ruptures. By M 6.6, at least one dip-slip step is larger than any of the strike-slip cases; and, by $M \sim 7.0$, dip-slip ruptures are capable of crossing steps of 10 km or more. Selected event numbers are shown to identify outer cases. Some events have multiple steps, indicated by fine connecting lines. The color version of this figure is available only in the electronic edition.

95% range of the normal parameter estimate (0.62 versus 0.22–0.52), and the best estimate for the normal step set, $p = 0.37$, is outside the 95% range for reverse steps (0.41–0.83). In light of the small numbers of events in the normal and reverse subsets, any use of their parameter estimates should also recognize their uncertainties.

Effect of Step Size on Rupture Propagation

In the geometric modeling section, all steps were of the interior type and thus broken during rupture. Additionally, the dimensions of steps were not distinguished except to be 1 km or greater. Here, we use the data summarized in the final columns of Tables 1 and 2 to develop a comparison data set of steps not broken by ruptures, with a goal to examine the effect of step size on rupture propagation. For parametric measurements at ends, we considered only those endpoints of rupture where fault mapping details are sufficient to characterize how the fault continues and the dimension of any step associated with the endpoint of rupture. The resulting data are displayed in Figure 9 as a plot of step size versus

rupture length. We find steps at a total of 31 strike-slip rupture ends and 7 dip-slip ends. Figure 9 offers no support for the idea that it takes a larger step to stop a larger earthquake.

Interior and ending step-size data from Figures 5 and 9 are summarized in Table 5. The summarization from Tables 1 and 2 into Table 5 consists of resolving the measured step-size observations in Tables 1 and 2 into whole kilometer bins. Any steps in Tables 1 and 2 with half-kilometer values (1.5, 2.5, ...) were divided equally between bounding bins. This step of concentration is required to allow us to meaningfully compare the frequencies of a given step size between the interior and ending data. For analysis, we include only steps 6 km or smaller.

The use of frequencies of incidence to investigate the effect of step size can be introduced with an example. If steps of a given size commonly end ruptures but that size rarely occurs inside them, we would have evidence that step size more efficiently stops ruptures. To convert entries in Table 5 to frequencies, we divide each column for ≤ 6 km by their totals, 26 for ending steps and 62 for interior steps. At rupture ends, six fall in the 1 km bin, for a fraction of 6/26, or 0.23. Interior steps of 1 km total 26, for a frequency of 26/62, or 0.42. Fractions constructed in this way are plotted in Figure 10a. Inspection of Figure 10 shows that a larger fraction of 1 km steps occur within ruptures than at their ends. The fractions are comparable for 3 km steps, and larger steps stop ruptures more often than they allow them to pass through.

To complete the comparison of step sizes, we divide the fractions for interior steps in Figure 10a by the corresponding fraction for steps at ends. We call the result, shown in Figure 10b, the “passing ratio,” because it expresses the ratio of interior (passed) step incidence to that of steps at endpoints of ruptures (not passed). The passing ratio has two useful end members. The passing ratio must diverge upward as step size approaches zero, because very small steps do not have the mechanical capacity to stop rupture. Similarly, there is almost certainly a step size so large that it cannot be crossed in a strike-slip rupture; for large steps, the passing ratio must approach zero. From these considerations alone, the passing ratio function must descend to the right in Figure 10b. The actual ratios (triangles) generally conform to this expectation. As intuition and fault mechanics would suggest, a small step is readily broken and a poor ending constraint, whereas large steps more frequently succeed in stopping rupture. Although the passing ratio cannot be linear for all step sizes,

Table 3
Interior Step Counts by Rupture Mechanism

Mechanism	Number of Events	Number of Interior Steps	Events with 0 Steps	Events with 1 Step	Events with 2 Steps	Events with 3 Steps	Events with 4 Steps	Events with 5 Steps	Events with > 5 Steps
All	76	94	26	29	10	6	2	2	1
Strike slip	46	62	16	15	7	5	1	1	1 (9 steps)
Normal	16	24	3	8	2	1	1	1	0
Reverse	14	8	7	6	1	0	0	0	0
Dip slip	30	32	10	14	3	1	1	1	0

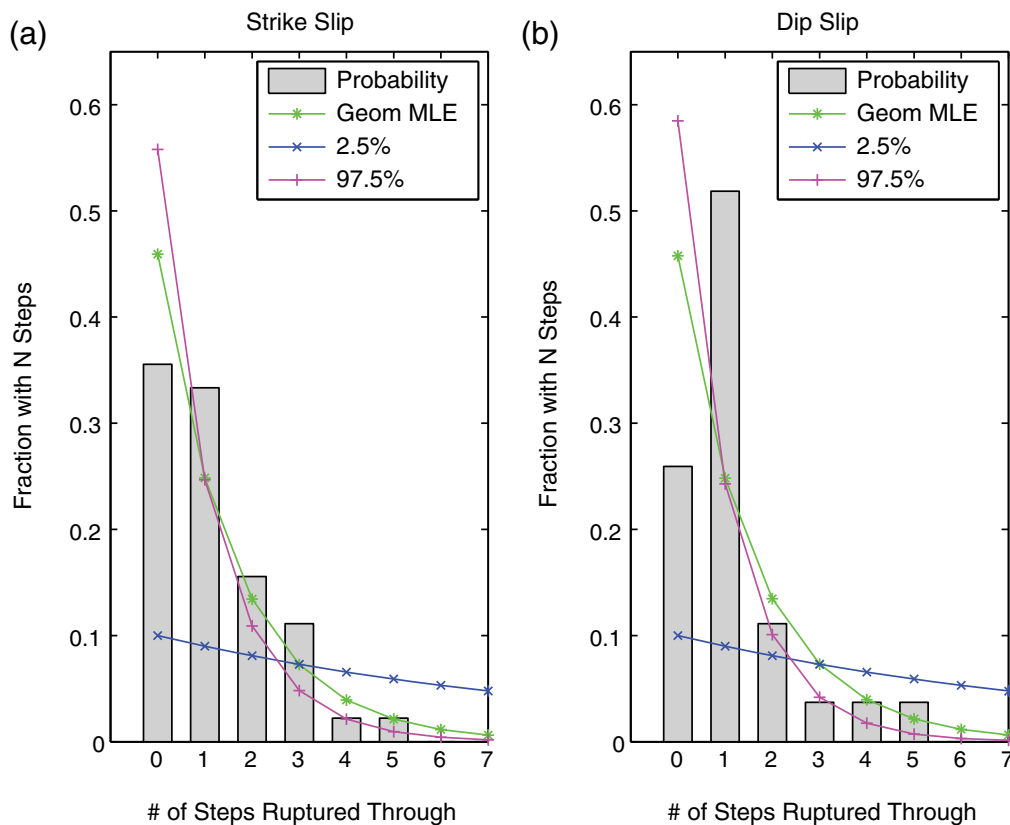


Figure 7. Distribution of the number of steps of 1 km or greater crossed by ground ruptures with (a) strike-slip and (b) dip-slip mechanisms. The strike-slip distribution summarizes 45 events and 53 steps. For dip slip, 27 ruptures > 10 km in length and 32 steps are included. For estimating the strike-slip geometric model parameter, the 1957 Gobi-Altai rupture with nine steps has been excluded. Geom MLE is the geometric model maximum likelihood estimate. Fit uncertainties at the 2.5% and 97.5% bounds are also shown. The color version of this figure is available only in the electronic edition.

we use a linear fit for steps from 1 to 6 km as the simplest way to summarize it. We find that steps from 1 to 6 km are passed with a ratio of $1.89-0.31 \times$ step width (in kilometers). From this line, steps of 3 km are approximately equal in tendency to stop ruptures or to be broken by them, and strike-slip ruptures are predicted to not pass through steps of 6 km or larger. Informal exploration of the linear trend shows that it is stable to reasonable permutations of the end step-size data set that might come from alternative interpretations of the surface rupture and fault mappings.

The comparative effectiveness of compressional versus extensional steps to stop ruptures has been a matter of active research (e.g., Harris and Day, 1993; Duan and Oglesby, 2006;

Lozos *et al.*, 2011). The subset of strike-slip mechanism events from our present data set (Tables 1 and 2) is large enough to investigate this question. Compressional steps might preferentially stop ruptures, because fault slip takes energy from rupture to create topography and because friction is greater for reverse components of a compressional system. On the other hand, extensional steps develop less frictional resistance to a dynamic stress pulse but may be less efficient at communicating dynamic energy across the step. Extensional steps within ruptures comprise 65% (40 of 62) but form a higher fraction of rupture ends, at about 81% (21 of 26, counting only steps ≤ 6 km). Compressional step fractions trend the opposite way. Within ruptures, they make up 35% (22 of 62), compared with only 19% on ends (5 of 26). Thus, the relative incidence of extensional steps goes up at rupture ends, and the fraction of compressional steps on rupture ends goes down. Acknowledging that sample sizes are small, this result suggests that extensional steps are somewhat more effective than compressional steps in stopping ruptures.

Table 4

Geometric Probability Parameters for Interior Steps Overcome by Ruptures

Mechanism	Geometric Probability	$p_{0.025}-p_{0.975}$
Strike slip	0.46	0.36-0.56
Normal	0.37	0.22-0.52
Reverse	0.62	0.41-0.83
Dip slip	0.46	0.33-0.58

$p_{0.025}$ and $p_{0.975}$ are the 2.5% and 97.5% confidence bounds, respectively, on the geometric probability parameter estimate.

Structural Discontinuities and Rupture Termination

The statistics of the geometric complexities associated with the endpoints of strike-slip ruptures are summarized in

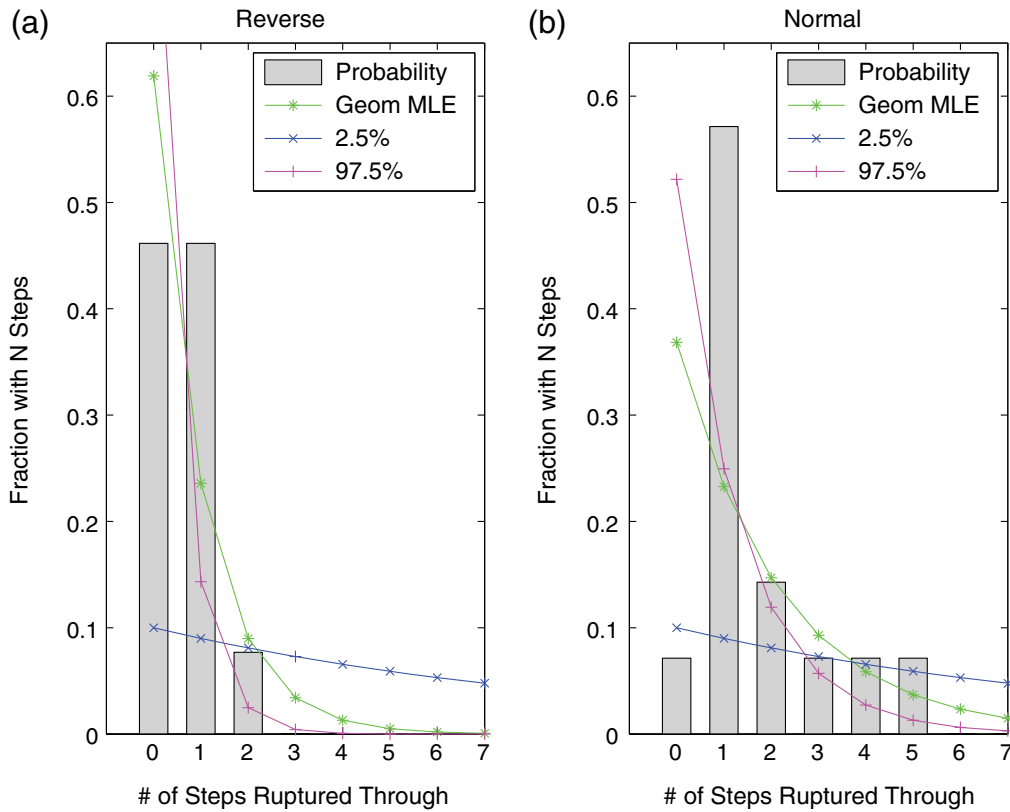


Figure 8. Separate distributions of the number of steps crossed in (a) reverse and (b) normal mechanism ruptures. The distributions include 13 events and 8 steps for the reverse case and 14 events and 24 steps for normal-faulting ruptures. Only ruptures longer than 10 km are included. Small sample sizes lead to large uncertainties in mean rates. Geom MLE is the geometric model maximum likelihood estimate. The color version of this figure is available only in the electronic edition.

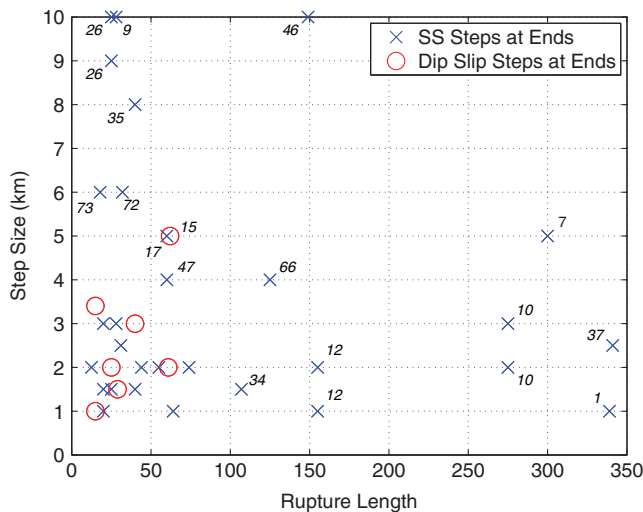


Figure 9. Step sizes at rupture ends are plotted versus surface rupture length. Event numbers from Tables 1 and 2 are shown for selected events. Steps at rupture end contrast with interior steps because they have stopped a rupture. There are fewer data than for interior steps because only a subset of faults have geologic mapping beyond the ends of ruptures sufficient to identify what, if any, structure caused rupture to stop. (SS, strike slip.) The color version of this figure is available only in the electronic edition.

histogram form in Figure 11. For this plot, we count all rupture ends for which mapping is sufficient to tell how the rupture end relates to active faults there (last column of Tables 1 and 2). The first three columns of the histogram represent the fraction of ends of ruptures where (1) rupture ceased even though the active fault trace continues, (2) rupture terminated at the end of a mapped active fault trace, and (3) rupture terminated at a step of 1 km dimension or greater. The fourth column is the sum of (2) and (3). Ruptures that end at the end of a fault or at a step comprise 69% of the strike-slip data. Ruptures that end where the fault continues comprise the remaining 31%. Combining these probabilities, a rupture with ends drawn at random from this distribution will float (i.e., neither end includes a step or fault end) only about

Table 5
Number of Steps Inside and Ending Ruptures Summarized on Whole-Kilometers Bins

Mechanism, Location	Step Size (km)						
	1	2	3	4	5	6	>6
Strike slip, interior	26	21	10	3	2	0	0
Dip slip, interior	7	6	5	4	2	0	8
Strike slip, ending	6	10	4	2	2	2	5
Dip slip, ending	2	2	2	0	1	0	0

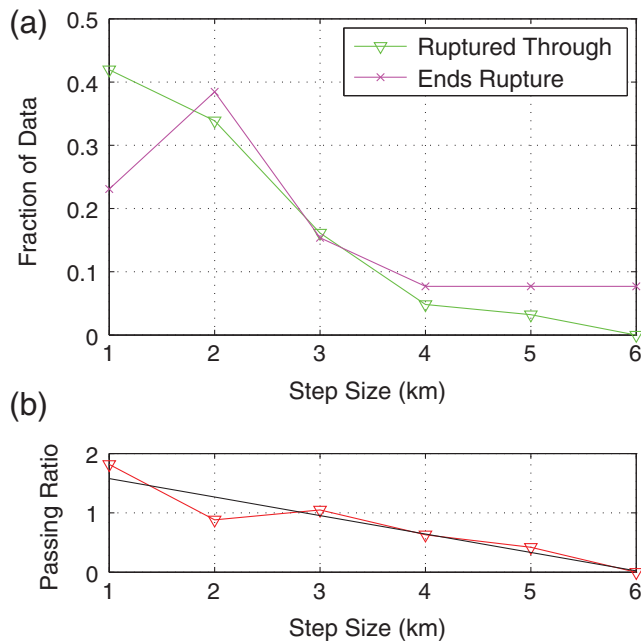


Figure 10. Comparison of steps inside ruptures to steps on ends for strike-slip ruptures. (a) The fractions of steps inside ruptures and steps ending ruptures are plotted as a function of step size. Steps of 1 km are broken more often than they arrest rupture, whereas 5 km steps predictably arrest rupture more often than they are broken through. None cross steps of 6 km. (b) The passing ratio is the ratio of the interior (broken) step and rupture end (effective) step fractions from (a). The linear fit is given by passing ratio $1.89 - 0.31 \times$ step size. Ruptures of about 3 km are predicted to stop ruptures or allow them to pass with roughly equal frequency. The passing ratio approaches zero for steps 6 km or more. The linear trend cannot continue for smaller step sizes because the ratio must diverge as step size approaches zero. The color version of this figure is available only in the electronic edition.

$0.31 \times 0.31 = 10\%$ of cases. Statistically then, our data predict that $\sim 90\%$ of strike-slip ruptures will have at least one end at a mappable structural discontinuity, and roughly $0.69 \times 0.69 = 48\%$ will have two.

Gaps in Rupture

The number and sizes of gaps along mapped earthquake ruptures are summarized for the combined data set and plotted as a function of earthquake magnitude and mechanism in Figures 12 and 13. Gaps occur in ruptures of all magnitudes and exhibit no obvious trend of frequency with length or earthquake size. Table 6 summarizes the fraction of earthquakes for which gaps in rupture trace were observed. Columns of the table include the total number of surface rupture maps for earthquakes of each respective fault mechanism, the number of those maps of sufficient quality to define gaps, the number of rupture maps displaying at least one gap of ≥ 1 km dimension, and the overall fraction of surface rupture maps with gaps. Overall, roughly 43% of surface ruptures include gaps of 1 km or more. The ratio for strike-slip ruptures, at 38%, is slightly lower than the 50% ratio observed for the combined set of dip-slip cases.

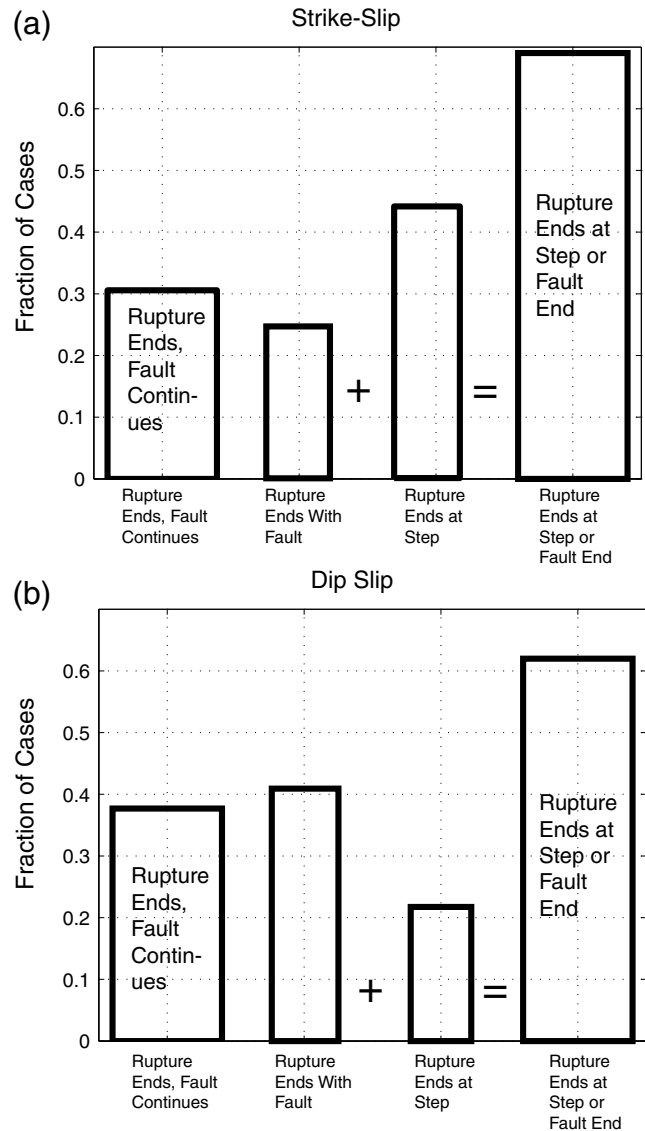


Figure 11. (a) Strike-slip and (b) dip-slip rupture ends. Three stopping categories are used: rupture ends but the fault continues (left bars), rupture ends with the end of the mapped fault, and rupture ends at a step of 1 km or larger. Fault end and step fractions are summed to form the rightmost bar. (a) In 31% of strike-slip rupture ends, the fault continues while the rupture stops. If fault ends are chosen randomly and follow these probabilities, floating ruptures with neither end at a geometric feature should occur roughly $0.31^2 = 10\%$ of the time. Cases in which ruptures end with the fault are less frequent than endings at a step, at 25% and 44%, respectively. (b) Dip-slip ruptures end with the fault more often (41%) and at steps less often (22%) than strike-slip ruptures.

Discussion

This study expands upon earlier studies by Wesnousky (2006, 2008), which provided an initial estimate of the maximum step size through which an earthquake might rupture. Observational bounds on rupture step size were used to evaluate potential fault-to-fault connections in the recent Uniform California Earthquake Rupture Forecast Version 3 (Milner *et al.*, 2013; Field *et al.*, 2014). The present ex-

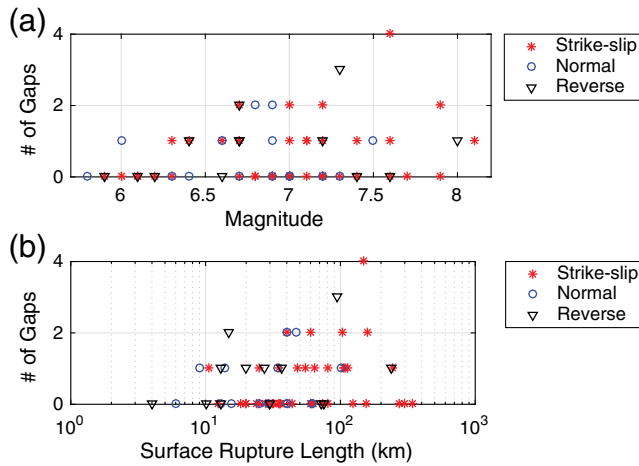


Figure 12. (a) The number of gaps in rupture traces shows no clear pattern when plotted versus magnitude. (b) When plotted versus length, we find that shorter dip-slip ruptures may more frequently include gaps than strike-slip ruptures of the same length. The number of gaps in traces increases somewhat with length in both types of ruptures, suggesting a modest dependence of gap incidence with length. The color version of this figure is available only in the electronic edition.

panded data set and analyses provide a number of new results that may be useful in future seismic-hazard analyses. New results may also contribute observational bounds on physical models of earthquake rupture phenomenology.

From our initial plot of the number of interior steps versus rupture length in Figure 4, we arrive at a number of first-order observations: (1) steps of 1 km or larger can occur in ruptures as short as 10 km; (2) dip-slip ruptures shorter than 25 km may be somewhat more likely to include steps than corresponding strike-slip cases; (3) the frequency of occurrence of steps in strike-slip and dip-slip ruptures is similar; and (4) for longer ruptures, there is no apparent relationship between rupture length and the number of interior steps. This last point seems to indicate that long ruptures may, but certainly do not always, grow by breaking through steps to add next segments on the fault.

The plots of step size versus rupture length and magnitude in Figures 5 and 6 show that dip-slip ruptures can incorporate larger steps than strike-slip earthquakes across the entire range of rupture lengths and magnitudes. Prospective uses of fault maps for estimating rupture sources and probabilities may be improved by taking this into account. The diagrams in Figure 14 are provided for discussion of the relationship of fault geometry to step size. Figure 14a and 14b are drawn for the normal-faulting dip-slip case, but the geometry approximately applies to reverse faults by reversing the direction of stress to cause regional shortening.

In both the normal and reverse-faulting cases, two features promote crossing larger steps. First is simple proximity. The rupture surfaces may be closer together at depth than they are at the surface, either because they have oppositely verging dips (Fig. 14a), or if the dip directions are the same, surfaces may be closer together than their surface trace by a geometric

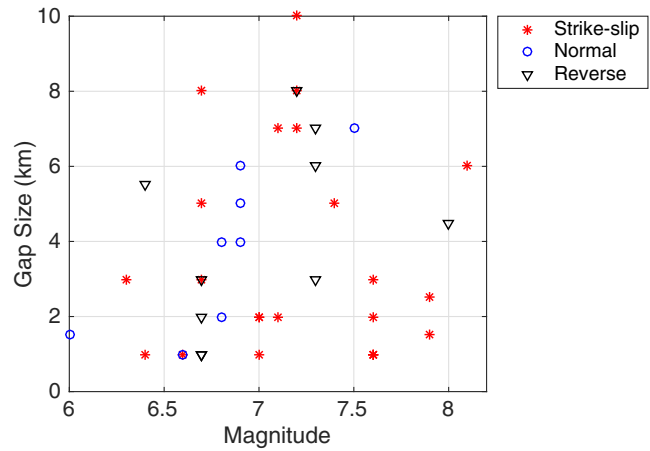


Figure 13. Gap sizes do not obviously correlate with earthquake magnitude or rupture mechanism. The color version of this figure is available only in the electronic edition.

correction $1-\cos(\text{dip})$ (Fig. 14b). Fault surfaces also may be closer at depth by any degree to which the faults converge at depth (Fig. 14b). The second factor favoring larger steps in dip-slip ruptures is that regional stresses promoting dip slip on a given fault will act to promote slip on other subparallel dip-slip faults potentially at some distance away. In extreme cases, the continuity of the common stress condition shared among faults is expressed during rupture as a “horsetail” or even an areal shattering of the upper crust (e.g., 1970 Gediz, Turkey; see the electronic supplement). Both the factors of continuity of stress and fault proximity at depth appear to have contributed to the unusual 2011 Iwaki, Japan, normal-faulting event. In contrast, stresses driving strike-slip faults do not intrinsically promote fault-perpendicular steps. *Lozos et al. (2011)* show that stresses favorably oriented to drive strike-slip rupture are not favorably oriented to promote slip on linking segments across steps.

In dynamic modeling, stress misalignment reduces the ability of ruptures to cross steps, and it limits the size of steps that can be crossed to a few kilometers. One solution for crossing steps would have the fault better aligned at depth but form a Y-shaped geometry as it extends upward to the surface (Fig. 14c). Friction considerations limit the separation of the Y at the surface to a few kilometers because the area in each arm of the Y, and thus force required for motion, increases with separation. Strike-slip faults that do not connect at depth (Fig. 14d) might, in principle, accommodate larger steps but require more complex faulting to accommo-

Table 6
Fraction of Events with Gaps of 1 km or Larger

Mechanism	Interpreted Events	Number with Gap ≥ 1 km	Fraction with Gaps
Strike slip	42	16	.38
Normal	15	7	.47
Reverse	13	7	.54
Dip slip	28	14	.50

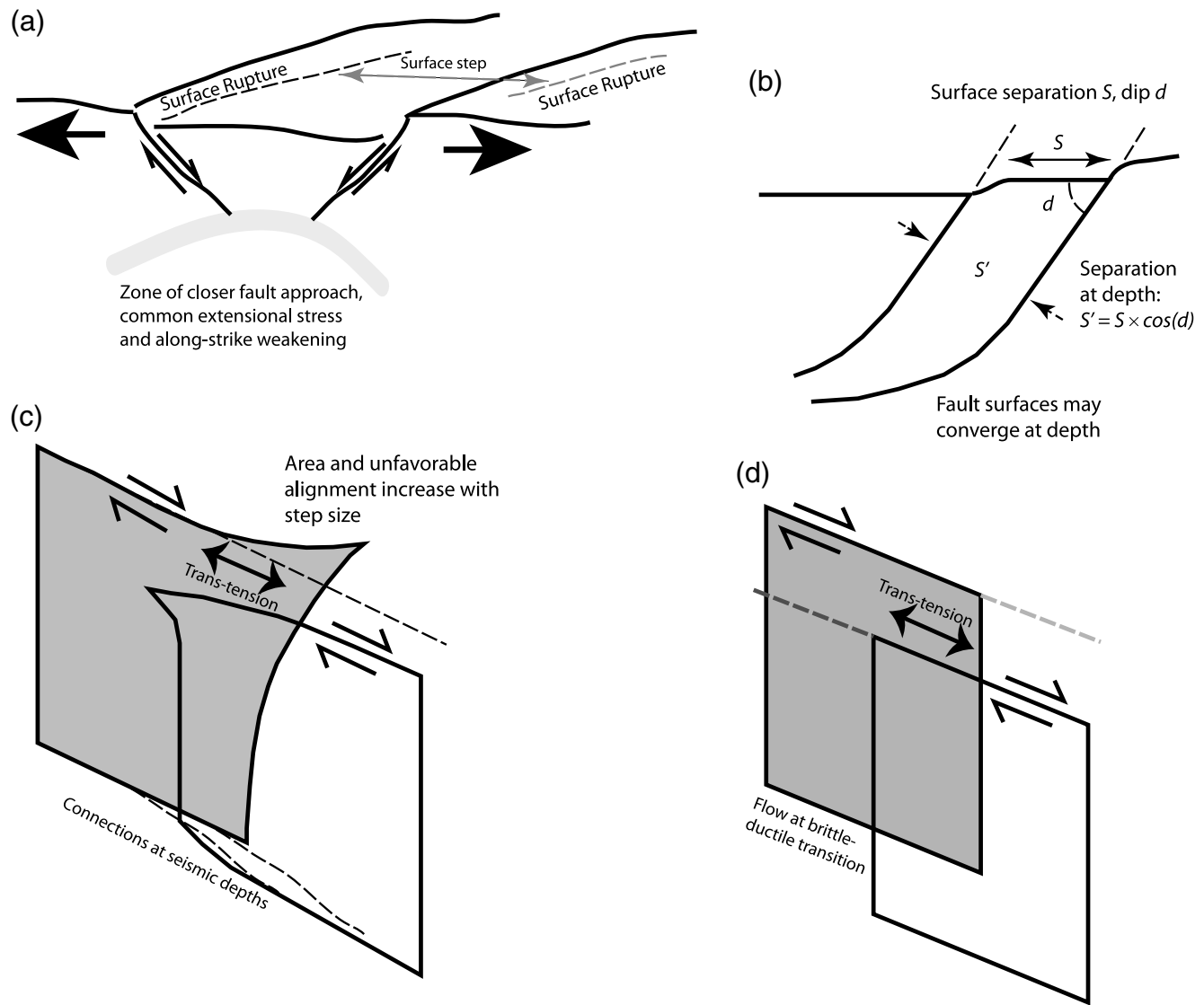


Figure 14. Potential reasons for the relative favorability of dip-slip step geometry for crossing larger steps. (a) Centrally vergent dip-slip faults are closer in the subsurface than their apparent separation at the surface. In addition, dilatational stress (large arrows) favoring slip on one fault promotes slip on others along strike. The reverse-mechanism case is geometrically similar but acts to shorten the section. (b) Dipping faults separated by S at the surface are separated by $S' = S \times \cos(d)$, in which d is the fault dip. Dip-slip faults can be closer at depth by up to $\sim 30\%$ by their geometry. They may also converge at depth, in the limit into a single common surface. (c) Strike-slip fault with a common (curving) trace at seismogenic depth. The step size is limited by the dimensions possible in a Y shape from a common base. (d) Idealized strike-slip step soling in the brittle–ductile transition without a common trace.

date relative displacements at depth. Conditions for continuance of the rupture through steps are a subject of ongoing research (Harris *et al.*, 1991; Harris and Day, 1993; Duan and Oglesby, 2006; Lozos *et al.*, 2011, 2015); however, empirically and in dynamic models, some threshold must be exceeded, perhaps conditioned by the stress history of the step (Duan and Oglesby, 2005), for the rupture to continue. From our data, steps in strike-slip ruptures of 4 km or larger occur in only about 8% of total cases.

We find (Fig. 7) that the expected number of steps in strike-slip ruptures is reasonably modeled by a geometric distribution. Ruptures most commonly have zero or one interior step and rarely have five or more. The geometric probability

distribution parameter value for strike-slip earthquakes of 0.46 is similar to the estimate of 0.49 developed by Wesnousky and Biasi (2011) from the events in Wesnousky (2008). Thus, steps of 1 km or more, when considered as an ensemble, are effective in stopping rupture about 46% of the time. In new results, the combined dip-slip data enable us to develop a corresponding estimate for dip-slip earthquakes. The resulting geometric parameter estimate of $p = 0.46$ is essentially identical to that for strike-slip events. In light of the differences in the stress regimes driving strike-slip ruptures, as compared with dip-slip ruptures, it is perhaps remarkable that the average rate at which steps are crossed is the same. When dip-slip events are divided into reverse and

normal mechanism groups, however (Fig. 8), we see that the agreement is only apparent. Steps in normal faults are less effective than the average in stopping ruptures, whereas steps in reverse faults are more effective. The probabilities developed in Figures 7 and 8 and summarized in Table 4 for dip-slip and strike-slip earthquakes may be useful in future studies to adjust probabilities of rupture length among scenario ruptures on a fault that includes steps.

The geometric distribution we used to model the frequency of steps in earthquake ruptures is more precisely described as an experiment with fixed probability that is repeated until a failure occurs. In our case, failure refers to the apparent inability of a rupture to cross a step. The model is a simplification of the actual earthquake process because the geometric model (as presented) treats one end as given and the expected number of steps as a geometric random variable governing expectations only for the other end. In spite of these simplifications, the model appears to give a reasonable assessment of the likelihood that a rupture considered at random will include any given number of steps.

To date, observations have been sufficient only to suggest an approximate upper limit of step size through which a strike-slip earthquake might rupture. In Wesnousky (2006, 2008), the largest strike-slip step broken in rupture was 4 km, implying a bound of 5 km. New observations summarized in Figure 6 show that steps of 5 km for strike-slip earthquakes can occur, but, in the combined strike-slip set, they together comprise only 3% of interior steps. A higher limit of about 10–12 km is suggested for dip-slip earthquakes. The declining fraction of the respective step observations formed by large steps suggests that while larger steps for both mechanisms may eventually be uncovered, their net frequency of occurrence should be very low.

We compliment the expanded data set of interior steps with a new compilation of step sizes ending ruptures. The combination (Figs. 5 and 9) provides the first observational basis to estimate the effect of step size on strike-slip rupture propagation (Fig. 10). Because of the large difference in sample size, the two data sets cannot be directly compared. However, the fraction of interior (broken) steps of a given step size can be compared to the fraction of steps of the same size associated with rupture termination. We refer to the ratio of these fractions as the passing ratio. Because of the small size of the end step data set, passing ratios for individual step sizes depend on one or a few observations, but, considered together, the passing ratio is seen to decrease systematically with increasing step size. The trend of the passing ratio line is also consistent with known end members. The effectiveness of a step to stop rupture must decrease and the passing ratio increase with step size below 1 km, because there is less and less structure in a small step to form an obstruction. As the other end member, there must be a largest step size through which no rupture can pass, at which point the passing ratio approaches zero. The passing ratio approaches zero for step size of about 6 km suggesting, consistent with Figure 6, that rupture through larger continental strike-slip steps should be

rare. The empirical data indicate that earthquake ruptures pass through or stop at steps of ~ 3 km with about equal probability and that smaller or larger steps are, respectively, less or more likely to stop ruptures. The results in Figure 10 provide an additional tool for seismic-hazard analysts to assign relative probabilities to rupture scenarios on a fault where the mapped trace includes steps. With less predictive power, we also find that ruptures are more often stopped by an extensional step than a compressional one. The passing ratio in Figure 10 and relative stopping ratios by step type provide empirical data of potential use in evaluating dynamic models of earthquake rupture propagation through steps (e.g., Harris and Day, 1993; Duan and Oglesby, 2006; Lozos *et al.*, 2011, 2015).

The composite surface rupture data set confirms that most rupture ends are influenced by geologic structures that might be mapped in advance. Among strike-slip ruptures, 69% of ends occur at a fault end or step of 1 km or larger. At 63%, dip-slip ruptures are slightly less likely to end at structural bounds but more likely by 41%–25% than strike-slip ruptures to end with a fault end. This difference is consistent with the mechanical differences of the slip mechanism. Where slip is parallel to strike, faults are mechanically disposed to continue, whereas dip-slip motion occurs perpendicular to strike, and fault ends face little by way of intrinsic mechanical inconsistency. We can also use the data to isolate the stopping tendencies of steps alone by removing the cases in Figure 11 in which a fault ends. In this subset, by $\sim 59\%$ and 37% , respectively, strike-slip and dip-slip rupture ends occur at steps. If strike-slip rupture ends are considered to be drawn at random from the distribution in Figure 11, ruptures in which neither end stops at a step or fault end comprise only about 10% of cases, and 90% of ruptures have at least one end at a mappable structural discontinuity (Fig. 11). Earthquake ruptures with neither end associated with a geometrical discontinuity are sometimes referred to as “floating.” Based on our data compilation, we can say that some earthquakes float, but most do not. By the same token, “characteristic” ruptures with both ends at a fault end or step structures are predicted about 48% and 39% of the time for strike-slip and dip-slip ruptures, respectively. Thus, perhaps not surprisingly, fault structural features are found to be useful for predicting relative probabilities among ruptures on a fault, but they are not entirely controlling.

Gaps in surface ruptures provide one measure of the distance across which rupture at depth is at least minimally connected without involving displacement at the surface. Finite-fault models of rupture commonly show regions where slip at depth is greater than near the surface (e.g., Mai and Thingbaijam, 2014). Such gaps might signal a local slip deficit that can be expected to recover to the net fault slip rate in some future event or perhaps the current rupture at depth is catching up to the action of a previous shallow rupture. Most of the ruptures in the data set were mapped within a short time after their occurrence, so we do not think that our compilation of gaps can be dismissed as simply an artifact of the mapping detail. If our collected surface rupture set can be considered representative, then Figure 13 provides an estimate of the frequency at which

gaps may be expected in future ruptures. The fact that dip-slip ruptures have a relatively higher incidence of gaps than in strike-slip ruptures is consistent with the difference in along-strike continuity inferred above from rupture ends. Our ensemble of surface rupture maps indicates that gaps in surface ruptures occur overall in about 43% of ruptures and that finite-fault rupture models with greater slip at depth than at the surface should not be unusual. In addition to providing observational constraints on the earthquake rupture process, the potential of gaps in the rupture trace may also be of interest in assessments of the likelihood of surface rupture affecting facilities such as pipelines that cross active faults.

Conclusion

Field observations and empirical measurements drawn from them provide a fundamental body of evidence with which to shape predictions about future ruptures. Lengths and relative probabilities of ruptures comprise a fundamental input to seismic-hazard analyses and risk estimates. Empirical data provide a basis for evaluating geological and computational models of earthquakes, ground rupture, and fault mechanics. The combined surface rupture data resolve systematic differences between strike-slip and dip-slip ruptures and rupture terminations. Short dip-slip ruptures are more likely than strike-slip to include steps. Dip-slip ruptures jump larger steps than do strike-slip earthquakes. Within dip-slip ruptures, steps ≥ 5 km comprise 30% of all steps, compared with only about 3% at ≥ 5 km for strike slip. By comparing fractions of compressional versus extensional steps inside versus ending strike-slip ruptures, we find that extensional steps are somewhat more effective at stopping ruptures. We also find a moderate size dependence in the effectiveness of steps to stop strike-slip ruptures. Steps of 3 km in strike slip either stop ruptures or are jumped with equal probability. A linear model of the passing ratio = $1.89 - 0.31 \times$ step width predicts that steps of 1 km are 1.6 times as likely to be jumped as to stop rupture, 5 km steps should be jumped only about a third of the time, and strike-slip steps of 6 km or more are not expected. Future data may show that the passing ratio is not truly linear; however, from our data, the linear trend is suggested as a summary useful for seismic-hazard analysis and comparison with dynamic models.

Data and Resources

Surface rupture maps and descriptions of earthquakes were gathered from published and publically available resources. Where used, centroid moment tensor magnitude estimates were obtained from the Global Centroid Moment Tensor Project database (www.globalcmt.org/CMTsearch.html; last accessed June 2015).

Acknowledgments

Support from National Science Foundation (NSF) Award Number 1213768 for this project is gratefully acknowledged. Comments from David Oglesby and two anonymous reviewers are gratefully acknowledged and led to significant improvements in the article. Alex Morelan helped compile rupture literature and drew first versions of many of the surface rupture maps. This article is Center for Neotectonics Studies Contribution Number 66.

References

- Duan, B., and D. D. Oglesby (2005). Multicycle dynamics of non-planar strike-slip faults, *J. Geophys. Res.* **110**, no. B03304, doi: [10.1029/2004JB003298](https://doi.org/10.1029/2004JB003298).
- Duan, B., and D. D. Oglesby (2006). Heterogeneous fault stresses from previous earthquakes and the effect on dynamics of parallel strike-slip faults, *J. Geophys. Res.* **111**, no. B05309, doi: [10.1029/2005JB004138](https://doi.org/10.1029/2005JB004138).
- Field, E. H., R. J. Arrowsmith, G. P. Biasi, P. Bird, T. E. Dawson, K. R. Felzer, D. D. Jackson, K. M. Johnson, T. H. Jordan, C. Madden, *et al.* (2014). Uniform California Earthquake Rupture Forecast, version 3 (UCERF3)—The time-independent model, *Bull. Seismol. Soc. Am.* **104**, 1122–1180.
- Harris, R. A., and S. M. Day (1993). Dynamics of fault interaction: Parallel strike-slip faults, *J. Geophys. Res.* **98**, 4461–4472.
- Harris, R. A., R. J. Archuleta, and S. M. Day (1991). Fault steps and the dynamic rupture process: 2-D numerical simulations of a spontaneously propagating shear fracture, *Geophys. Res. Lett.* **18**, 893–896.
- Klinger, Y., M. Etchebes, P. Tapponnier, and C. Narteau (2011). Characteristic slip for five great earthquakes along the Fuyun fault in China, *Nat. Geosci.* **4**, 389–392.
- Larson, H. J. (1982). *Introduction to Probability Theory and Statistical Inference*, Third Ed., John Wiley and Sons, New York, 637 pp.
- Lozos, J. C., D. D. Oglesby, J. N. Brune, and K. B. Olsen (2015). Rupture propagation and ground motion of strike-slip stepovers with intermediate fault segments, *Bull. Seismol. Soc. Am.* **105**, 387–399.
- Lozos, J. C., D. D. Oglesby, B. Duan, and S. G. Wesnousky (2011). The effects of double fault bends on rupture propagation: A geometrical parameter study, *Bull. Seismol. Soc. Am.* **101**, 385–398.
- Mai, P. M., and K. K. S. Thingbaijam (2014). SRCMOD: An online database of finite-fault rupture models, *Seismol. Res. Lett.* **85**, 1348–1357.
- Milner, K. R., M. T. Page, E. H. Field, T. Parsons, G. P. Biasi, and B. E. Shaw (2013). Defining the inversion rupture set using plausibility filters, *U.S. Geol. Surv. Open-File Rept. 2013-1165*, Appendix T, 14 pp.
- Shi, J., X. Feng, S. Ge, Z. Yang, M. Bo, and J. Hu (1984). The Fuyun earthquake fault zone in Xinjiang, China, *Seismol. Press* **19**, 325–346.
- Wells, D. L., and K. J. Coppersmith (1994). New empirical relationships among magnitude, rupture length, rupture width, rupture area, and surface displacement, *Bull. Seismol. Soc. Am.* **84**, 974–1002.
- Wesnousky, S. G. (2006). Predicting the endpoints of earthquake ruptures, *Nature* **444**, 358–360.
- Wesnousky, S. G. (2008). Displacement and geometrical characteristics of earthquake surface ruptures: Issues and implications for seismic-hazard analysis and the process of earthquake rupture, *Bull. Seismol. Soc. Am.* **98**, 1609–1632.
- Wesnousky, S. G., and G. P. Biasi (2011). The length to which an earthquake will go to rupture, *Bull. Seismol. Soc. Am.* **101**, 1948–1950.

Nevada Seismological Laboratory
University of Nevada Reno
Mail Stop-174
Reno, Nevada 89557
glenn@unr.edu
wesnousky@unr.edu

Manuscript received 24 February 2016;
Published Online 24 May 2016